

Supporting Information

Kato et al. 10.1073/pnas.1120791109

SI Materials and Methods

Cell Culture. The BL2 Burkitt's lymphoma cell line was cultured in RPMI medium 1640 containing 10% FCS (vol/vol), 100 µM NEAA (Gibco), 1 mM sodium pyruvate, 100 units per mL penicillin, and 100 µg/mL streptomycin. BL2-ΔC-AIDER cells, which are a BL2 clone harboring Jp8BdelER (Jp8Bdel fused with the hormone-binding domain of the estrogen receptor [ER]), were cultured with 0.5 µg/mL puromycin. To activate AIDER proteins, 4-hydroxytamoxifen (4-OHT) was added to a concentration of 1 µM.

Microarray. DNA was labeled according to the Affymetrix sample preparation protocol and hybridized to Human Promoter 1.0R Arrays. Slides were scanned with an Affymetrix GeneChip scanner. Six independent experiments were performed for each sample. Microarray data were analyzed using CisGenome.

Analysis of Microarray Data. Normalized signal intensities were generated from Affymetrix CEL files using CisGenome (1). The parameters used to detect peaks are as follows: moving average (MA) is used to combine neighboring probes, false discovery rates is estimated from permutation test, the window boundary is set to 250 bp, the MA cutoff is set to 3, the max allowable gap within a region is set to 200 bp, the max run of insignificant probes with a region is set to 5, the minimum region length is set to 150 bp, and the minimum number of significant probes within a region is set to 5. We retained only peaks where the FDR is <0.3. All probe sequences were mapped to the hg19 genome assembly.

SOLiD Sequencing. Templated microbeads were prepared according to Applied Biosystem's standard protocol. Sequencing runs were performed on the SOLiD 3 Plus system (Applied Biosystems) under standard conditions.

Analysis of SOLiD DNA-Sequencing Data. Linkers were removed from the sequenced tags by using a custom Perl script, and the resulting tags were mapped to the human genome (assembly hg19) using the Bowtie program with standard parameters (2). Breakage points were summed over 100-bp intervals across the entire genome in 10-bp increments for each control and 4-OHT-treated replicate. Significant differences in breakage frequency were calculated using the EdgeR program (3), with background dispersion values for both conditions calculated over shifting 10,000-bp intervals. This program provided *P* values and FDR values for each 100-bp interval, measuring the likelihood of observing the differences in breakage points across the two conditions given the selected background breakage rates. Regions with low FDR values overlapping the promoter (defined as 500 bases upstream of the RefSeq-defined transcriptional start site) and gene definitions were extracted. To increase confidence in the potential AID targets, regions with significant *P* values were clustered via a single-linkage clustering procedure, which joined any regions within 1 kb of another peak on the genome. The resulting clusters of regions were then overlaid with low-FDR regions, and the most promising candidate genes containing the lowest FDR values (FDR < 0.1), high numbers of *P* value clusters, or both were selected for further validation testing (Table S2). This layer of additional clustering was chosen to facilitate the testing of genes with the highest likelihood of breakage. Indeed, both the *MALAT1* and *SNHG3* loci (Fig. S3A) displayed these patterns,

which were likely to be consistent with high levels of AID-induced cleavage activity.

Statistical Parameters of SOLiD DNA-Sequencing Data. In terms of data integrity, our technique is consistent with existing technologies. A summary of the characteristics of the sequenced libraries is provided in Table S8. The read redundancy ranges between 1.23 and 1.28; this redundancy rate is slightly higher than most ChIP-seq experiments (1.05–1.15) but much lower than other sequencing technologies. The slightly higher redundancy rates likely result from high numbers of breakages found in repeat regions (Fig. S5A). Importantly, the low redundancy values argue against problems arising from the number of cycles used, indicating the library does not suffer from amplification bias. An overview annotating the genomic locations of breakage sites in each library is also provided (Fig. S5B). The source of the discrepancies in target identification between this dataset and others instead likely stems from lack of depth. Each sequenced library covers the entire genome at roughly 0.8× coverage. Although the coverage of the as-currently undefined AID-targeted “break-ome” is not known, at present coverage levels, it appears possible to detect regions that are substantially affected by AID-induced breakage while not capturing everything that has been identified.

We have plotted the distribution of the square root of the absolute common dispersion values across the two conditions in all local genome windows which were used to approximate local background breakage rates for comparisons across samples (Fig. S5C). Very few genomic regions exceed an expected error rate of 20% in the measurements. We observe a bimodal distribution in the error rates, with the first peak corresponding to extremely low expected error (<1%) and the second peak found between ≈1–20%. The bimodal distribution implies that the AID breakage in a subset of genome regions is more highly reproducible relative to other regions; interestingly, this is not derived from relative expression values in the two peaks. Regardless, in either peak region the error rates are consistent with existing deep-sequencing techniques and enable robust identification of significant differences between breakage counts across conditions.

Mutation Analysis. To analyze SHM mutations, BL2-ΔC-AIDER cells were treated with 4-OHT (1 µM) for 24 h, and the genomic DNA was purified by phenol:chloroform extraction. PCR was performed by using *Pyrobest* or PrimeSTAR GXL DNA polymerase (TaKaRa) with the following amplification conditions: 95 °C for 5 min, 30 cycles at 95 °C for 30 s, 58 °C for 30 s, and 68 °C for 1 min. After purification, the PCR fragments were A-tailed and cloned with the pGEM-T Easy Vector System (Promega). Nucleotide sequences were determined with the ABI PRISM 3130xl Genetic Analyzer (Applied Biosystems). Only unique mutations were counted, and the mutation frequency was calculated from the number of mutations per total bases analyzed.

REPFIND Analysis. Analysis with the REPFIND Web server (<http://zlab.bu.edu/repfind/form.html>) used the following parameters: *P* value cutoff, 0.0001; minimum repeat length, 3; maximum repeat length, infinity; low complexity filter, on; statistical background, query sequence; order of background Markov model, 1.

ChIP. ChIP was performed as described (4).

1. Ji H, Wong WH (2005) TileMap: Create chromosomal map of tiling array hybridizations. *Bioinformatics* 21:3629–3636.
2. Langmead B, Trapnell C, Pop M, Salzberg SL (2009) Searching for SNPs with cloud computing. *Genome Biol* 10:R25.
3. Robinson MD, McCarthy DJ, Smyth GK (2010) edgeR: A Bioconductor package for differential expression analysis of digital gene expression data. *Bioinformatics* 26:139–140.
4. Stanlie A, Aida M, Muramatsu M, Honjo T, Begum NA (2010) Histone3 lysine4 trimethylation regulated by the facilitates chromatin transcription complex is critical for DNA cleavage in class switch recombination. *Proc Natl Acad Sci USA* 107: 22190–22195.

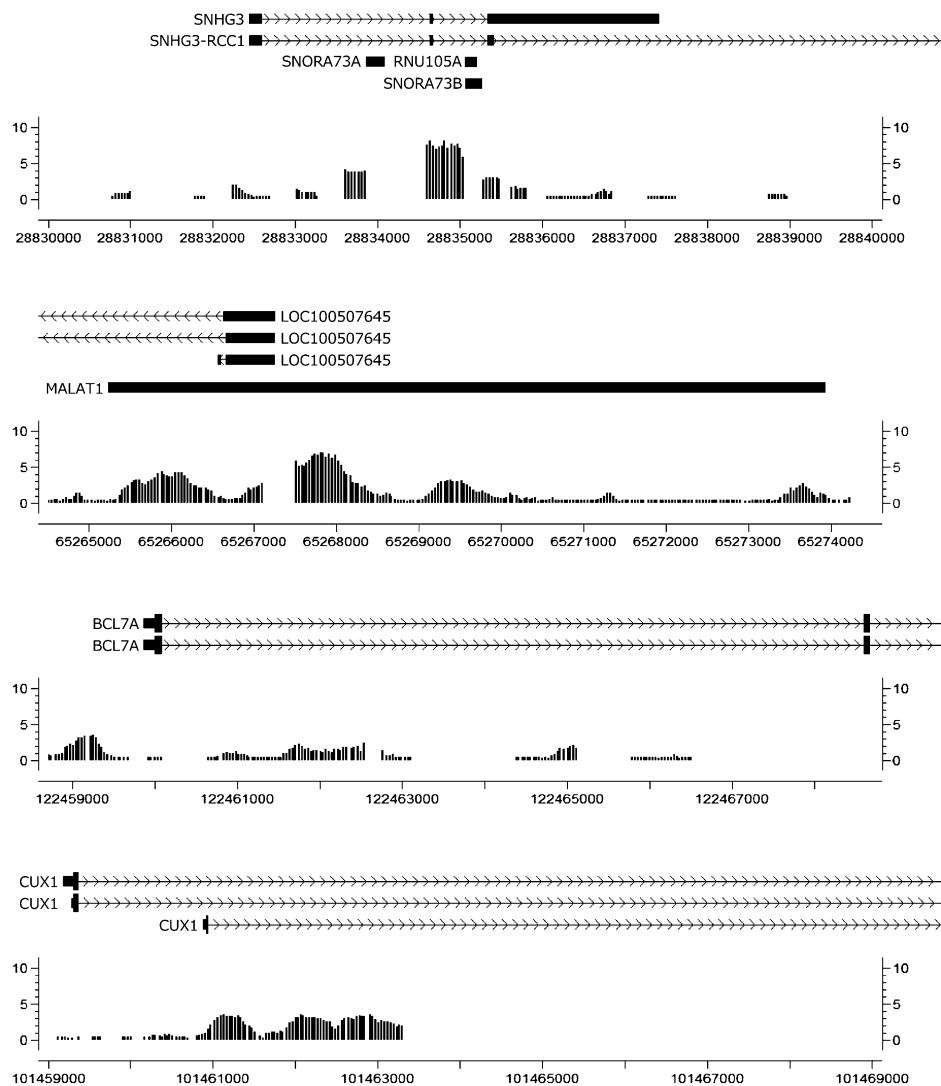


Fig. S1. Breakage signal distribution detected by promoter array. A 10-kb segment in the vicinity of detected breakage region is represented for each locus. Regions without array bars do not have array probes. x axis numbers indicate base positions according to hg19 assembly.

MYC

GGTGAAGGGTGCCTCTTATTCCCCACCAAGACCACCCAGCGCTTAGGGGATAGCTCTGCAAGGGAGAGGTTGGACT
 GTGGCGCGCACTGCGCGCTGCGCCAGGTTCCGCACCAAGACCCCTTAACACTAAGACTGCCTCCGCTTGTCGCCCCGCTCC
 AGCAGCCTCCCGCACGATGCCCTCAACGTTAGCTTCACCAAGCCAAGACTAGACCTCGACTACGACTCGGTGAGCGTATTT
 CTACTGCGACGAGGAGAGAACTCTACAGCAGCACAGCAGGGAGCTGAGGCCGGCCAGCGAGGATATCTGGA
 AAATTCGAGCTGCTGCCACCCGCCCTGTCCCCTAGCCGCCCTCGGGCTCTGCTGCCCTCTACGTTGGTCACACCCCT
 TCTCCCTGGGGAGACAACGACGGGGTGGGGAGCTCTCACGGCCGACCAGCTGGAGATGGTACCGAGCTGGAGG
 AGACATGGTAACCAGAGTTCATCTGCGACCCGACGAGACCTTCATCAAAACATCATCCAGGACTGTATGTGGAGC
 GGCTCTCGGCCGCCAACGCTCGTCTCAGAGAAGCTGCCCTACCGAGCTGCGCAGAACAGCGGAGCCGAACCCCG
 CCCGGGCCACAGCCTGCTCCACCTCAGCTTGACCTGAGGATCTGAGCGCCGCCCTAGAGTGCATCGACCCCTGGT
 GGTCTCCCTACCCCTCAACGACAGCAGCTGCCAAGTCCTGCGCCTCGAAGACTCCAGCGCTTCTCCGATCG
 TCTCTGCTCTCGACGGAGTCCTCCCGAGGGCAGCCCTGGTGCTCCATGAGGAGACACCGCCACCACAGCA
 GCGACTCTGGTAAGCGAAGCCCG

SNHG3

ATGATGATAAGTAGCTGGAGGAAGGAGAATCGCTGGAGCCAGGAGTGCCTATAACTCAAACCTATACTCCAGTGCCTACT
 CCAACCCAGCGATAGCATGAGGCCCTCGTTGAAAAGTTAGGTTTGCTGACTAATAGATTAATCTTGTGGAG
 ATTGTTAAGGATTCAAGTAACTCTTTGGTAGATAATCTGTAATTGTTTGCTTACGCTTGTCAATGATTTC
 TGTAATGAAATAGGATTGAAGAGACTTTTATTCTAGTTGGTCAGGATTACCTCTGAGGCATTAATCTCAGAGCAATAG
 CCAAAATCGACTTGTGCATTTGTAGGCATGTTGACATAACTCAACATATGCTCTGTTGTAAAAATTGCTTTTAG
 TCAGCTCATAAAAGTGCAGTAGTAAAGCTGCCCTAGTGAACGTAGGAAGCCTAATTGGCTTATCTACATGTGAGCCTG
 AGCTGAGAAAGATACTAGCCCTGAAAGTAGTAAAGCTGCCCTAGTGAACGTAGGAAGCCTAATTGGCTTATCTACATGTGAGCCTG
 GCATTCACGTGGATACCTGGAGGTCACTCTCCCAGGCTCTGCAAGTGGCATAGGGAGCTTAGGGCTGCCCCATGA
 TGACAGTCCTTCCACAACGTTGAAGATGAAGCTGGCCTCGTCTGCCCTGCATATTCCACAGC

Fig. S2. (Continued)

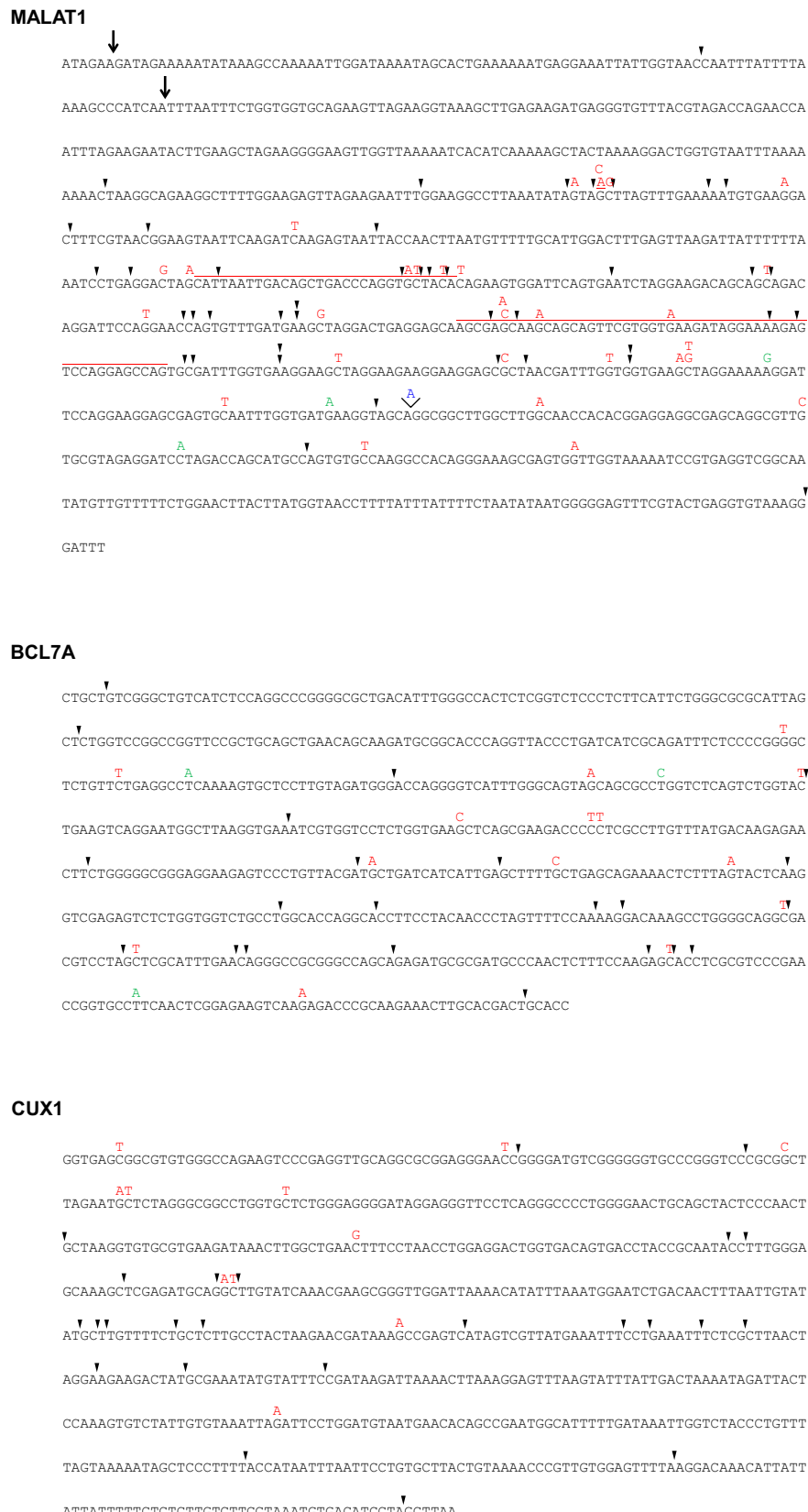


Fig. S2. Somatic mutations and breakpoint distribution in AID target loci. Red, mutations found in cells treated with 4-OHT for 24 h; green, mutations in 4-OHT nontreated samples; blue, insertions; red line, deletions; arrowheads, break sites in samples treated with 4-OHT for 3 h; arrows, translocation breakpoints shown in Fig. 3.

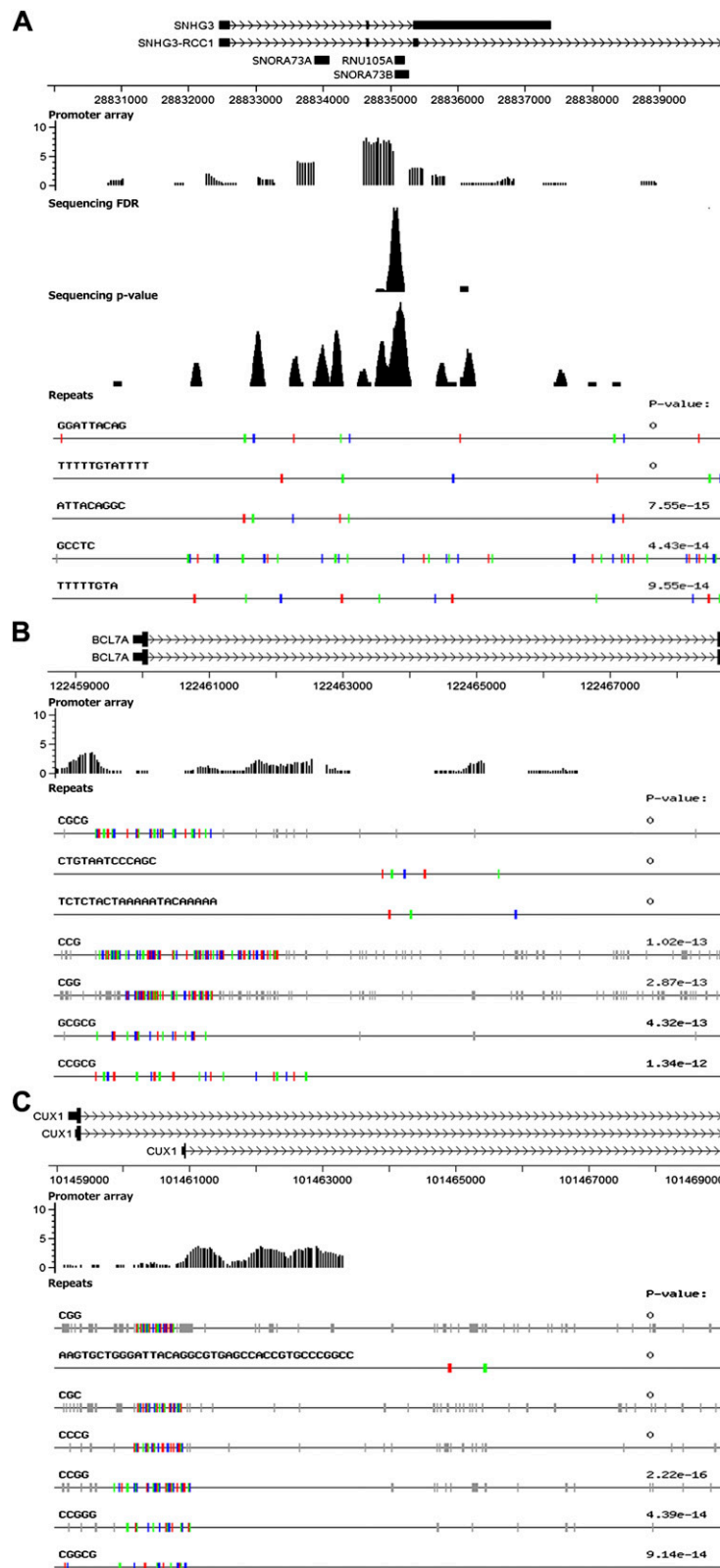


Fig. S3. Repeat sequences surrounding the breakage region in AID target genes. (A) *SNHG3* gene. From top to bottom: Representation of a 10-kb segment surrounding the *SNHG3* locus; Breakage signal distribution detected by promoter array (regions without bars do not have array probes); FDR regions by sequencing; *P* value peaks by sequencing; REPFIND analysis showing significant repeat clusters in the *SNHG3* locus. (B and C) *BCL7A* and *CUX1* genes, respectively. From top to bottom: Representation of a 10-kb segment surrounding the cleavage region for each gene; Breakage signal distribution detected by promoter array (regions without bars do not have array probes); REPFIND analysis showing significant repeat clusters in the same region. Motifs depicted as vertical small colored bars indicate the cluster with the most significant *P* value; individual repeats are separated by different colors. *x* axis numbers indicate base positions according to hg19 assembly.

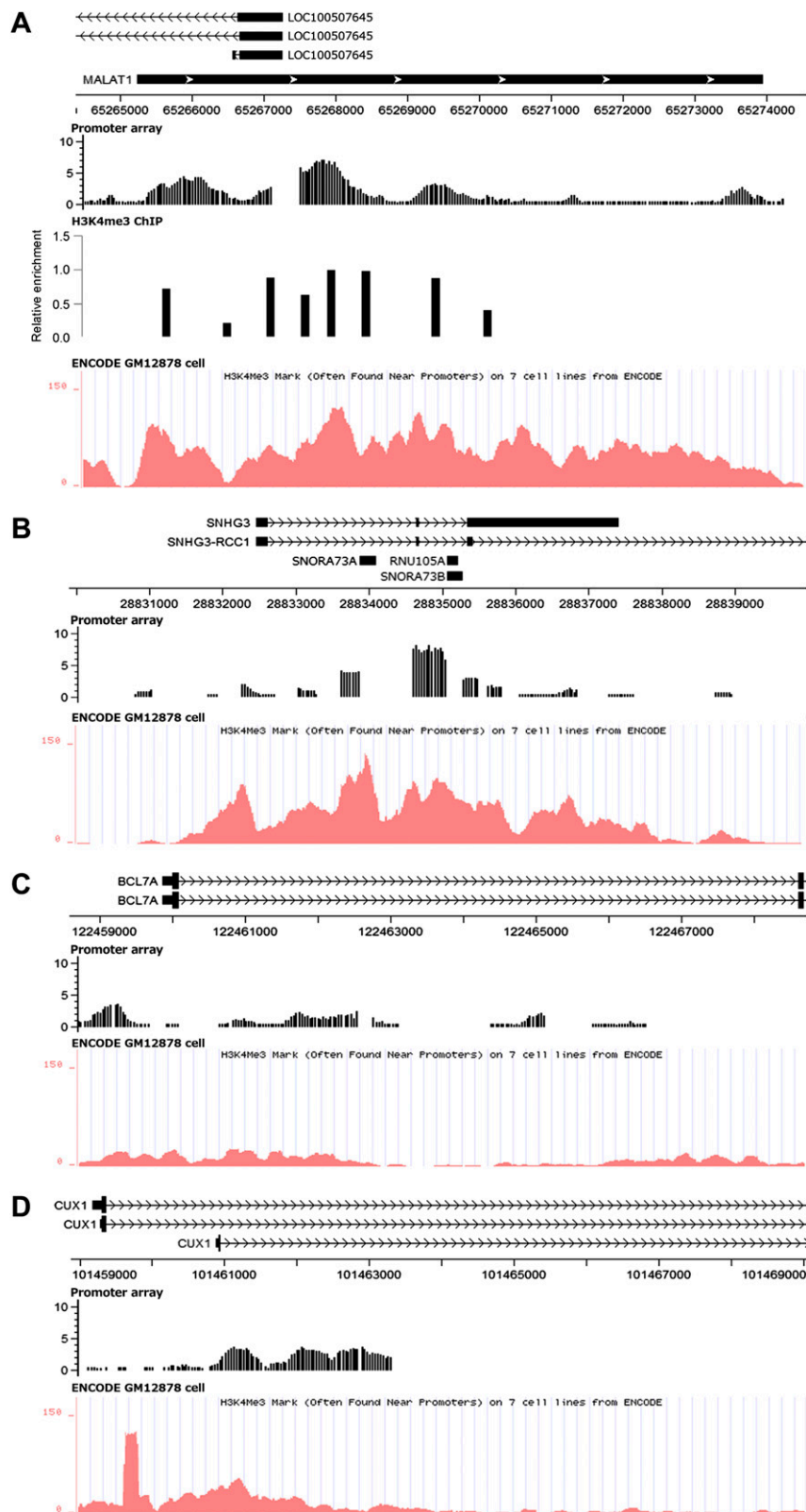


Fig. S4. H3K4me3 distribution in AID target genes. (A) *MALAT1* gene. From top to bottom: Representation of a 10-kb segment surrounding the *MALAT1* locus; Breakage signal distribution detected by promoter array (regions without bars do not have array probes); ChIP assay using an anti-H3K4me3 antibody; H3K4me3 status from ENCODE ChIP-seq data for GM12878 cell line. (B–D) *SNHG3*, *BCL7A* and *CUX1* genes, respectively. x axis numbers indicate base positions according to hg19 assembly.

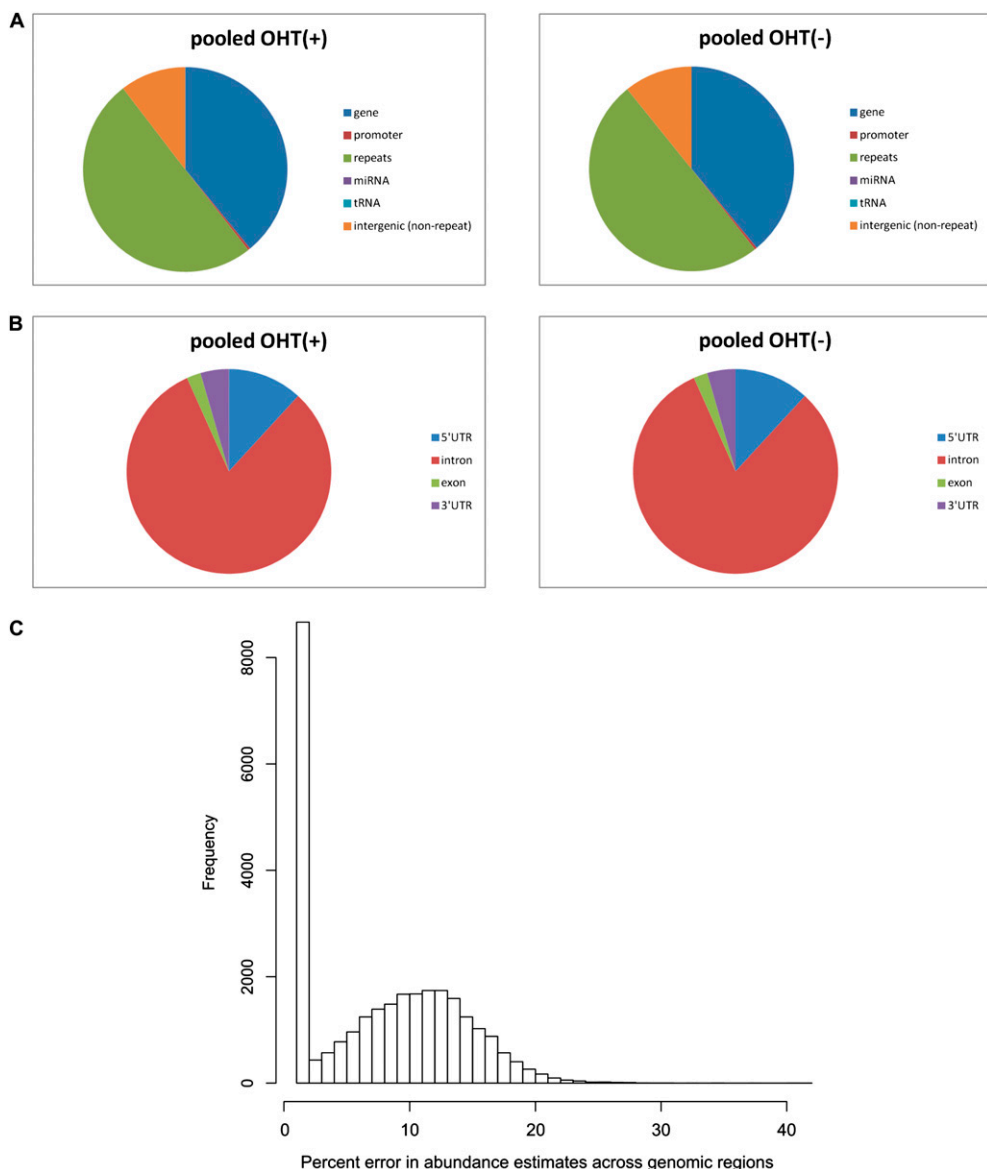


Fig. S5. Location of all mapped reads according to genome features (A) and distribution of gene-mapping reads to genomic locations (B). (C) Distribution of estimated percent error in abundance measurements across all analyzed genomic segments. The estimated percent error in breakage rates rarely exceeds 15–20%, enabling robust determination of significant differences.

Table S1. AID targets identified by promoter assay

Gene	Chromosome	Expression	Tilemap maxM/P	FDR value	Validation by qPCR	Translocation (partner gene)
<i>SNHG3</i>	chr1	+	8.18	0	+	CML (<i>PICALM</i>)
<i>MALAT1</i>	chr11	+	7.05	0	+	Renal cell carcinoma (<i>TFEB</i>), mesenchymal hamartoma of the liver (<i>ACAT2</i>)
<i>NIN</i>	chr14	+	6.25	0.08	—	CML-like myeloproliferative disorder (<i>PDGFRB</i>)
<i>FYB</i>	chr5	—	6.25	0.08	n.d.	—
<i>C2orf16</i>	chr2	—	6.05	0.1	—	—
<i>C9orf72</i>	chr9	+	5.93	0.11	—	—
<i>FAM119B</i>	chr12	—	5.62	0.2	n.d.	—
<i>CFLAR</i>	chr2	+	5.47	0.26	+	—
<i>SNX25</i>	chr4	+	5.45	0.26	—	—
<i>BCL7A</i>	chr12	+	3.53	0.83	+	Burlitt lymphoma (IgH; <i>MYC</i> -IgH)
<i>CUX1</i>	chr7	+	3.51	0.83	+	TLL (<i>FGFR1</i>)

FDR < 0.3 plus *BCL7A* and *CUX1*. Chr, chromosome; CML, chronic myeloid leukemia; n.d., not done; TLL, T-lymphoblastic leukemia/lymphoma.

Table S2. AID targets identified by sequencing

Gene	Chromosome	Expression	FDR value	P value clustering*	Validation by qPCR	Translocation (partner gene)
<i>MALAT1</i>	chr11	+	0.027	12	+	Renal cell carcinoma (<i>TFEB</i>), mesenchymal hamartoma of the liver (<i>ACAT2</i>)
<i>SNHG3</i>	chr1	+	0.015	9	+	CML (<i>PICALM</i>)
<i>SIPA1L3</i>	chr19	+	0.015	5	—	—
<i>KCNC2</i>	chr12	—	0.005	4	—	—
<i>ZNF451</i>	chr6	+	0.038	4	—	—
<i>TRIO</i>	chr5	+	0.050	4	—	—
<i>C5orf13</i>	chr5	+	0.072	4	—	—
<i>CUL9</i>	chr6	+	0.077	4	—	—
<i>TM9SF4</i>	chr20	+	0.026	3	—	—
<i>ANKRD11</i>	chr16	+	0.041	3	—	—
<i>MYO3B</i>	chr2	—	0.082	3	—	—
<i>UPF2</i>	chr10	+	0.093	3	—	—
<i>MET</i>	chr7	—	0.000	2	—	Gastric carcinoma (<i>TPR</i>)
<i>AUTS2</i>	chr7	+	0.017	2	—	ALL (<i>PAX5</i>)
<i>RAD18</i>	chr3	+	0.038	1	—	—
<i>OTUD6B</i>	chr8	+	0.041	1	n.d.	—
<i>VPS13B</i>	chr8	+	0.044	1	—	—
<i>CCDC41</i>	chr12	+	0.055	1	—	—
<i>ECT2</i>	chr3	+	0.078	1	—	—
<i>MRPL49</i>	chr11	+	0.020	1	—	Close to t(11;17)(q13;q21) translocation in B-NHL
<i>NECAB3</i>	chr20	+	0.029	1	—	—
<i>SETD8</i>	chr12	+	0.175	1	—	—
<i>SETBP1</i>	chr18	—	0.134	9	—	—
<i>PBLD</i>	chr10	—	0.254	8	—	—
<i>ABCG2</i>	chr4	—	0.220	8	—	—
<i>FAM65B</i>	chr6	+	0.195	8	—	—
<i>WBSCR17</i>	chr7	—	0.162	8	—	—
<i>ERC1</i>	chr12	+	0.153	6	—	—
<i>PLD2</i>	chr17	+	0.102	5	—	—

FDR < 0.1 and/or remarkable numbers of P value clusters. ALL, acute lymphocytic leukemia; B-NHL, B-cell non-Hodgkin lymphoma; Chr, chromosome; CML, chronic myeloid leukemia; n.d., not done.

*Number of P value clusters corresponding to the FDR region.

Table S3. Mutation analysis of genes with significant increase in break signal after AID activation

	4-OHT	Mutated clone	Unique mutations, bp	Total sequenced, bp	Mutation frequency ($\times 10^{-4}$)	del(ins) (bp)	Del(ins)/total clones	P value
<i>B2M</i>	—	1/82	1	43,674	0.23	0	0/82	0.52
	+	2/87	2	46,338	0.43	1	1/87	
<i>Sμ</i>	—	13/82	17	67,404	2.52	1	1/82	4.2×10^{-7}
	+	38/79	59	64,938	9.09	33(1)	7(1)/79	
V region	—	18/123	21	92,127	2.28	6	5/123	0.001
	+	38/135	51	101,115	5.04	8(10)	4(1)/135	
<i>MYC</i>	—	5/83	5	41,251	1.21	0	0/83	1.8×10^{-7}
	+	21/80	33	39,760	8.30	0	0/80	
<i>SNHG3</i>	—	3/77	3	42,633	0.70	0	0/77	0.0001
	+	16/74	21	41,170	5.10	2	2/74	
<i>MALAT1</i>	—	3/89	3	48,950	0.61	0	0/89	8.1×10^{-7}
	+	19/90	30	49,500	6.06	83(1)	3(1)/90	
<i>BCL7A</i>	—	3/84	3	44,520	0.67	0	0/84	0.006
	+	9/82	14	43,460	3.22	0	0/82	
<i>CUX1</i> *	—	0/89	0	48,149	0	0	0/89	0.001
	+	8/91	11	49,231	2.23	0	0/91	
<i>CUX1</i> †	—	13/85	14	58,905	2.38	0	0/85	0.007
	+	22/84	31	58,212	5.33	4	4/84	
<i>CFLAR</i>	—	0/134	0	87,404	0	5	1/134	0.004
	+	5/133	8	86,878	0.92	1	1/133	

Cells were treated with or without 4-OHT for 24 h. P values were calculated by one-sided Fisher's exact test.

*Region detected by promoter array (Fig. S2).

†Region with highest peak of H3K4me3 (Fig. S4D).

Table S4. Linker sequences

Linker primers (5' to 3')	
Linker P1	biotin - TTCCACTACGCCCTCGCTTCTCTATGGCAGTCGGTGT ATCACCGACTGCCCATAGAGAGGAAGCGGAGGCAGTT
Linker P2	AGAGAATGAGGAACCCGGGCAGTT CTGCCCCGGGTTCTCATTCCT
Global amplification (fwd)	CCACTACGCCCTCGCTTCTCTATG
(rev)	CTGCCCCGGGTTCTCATTCCT
P1-LM (LM-PCR)	CCACTACGCCCTCGCTTCTCTATG

Table S5. Gene-specific primers (5' to 3')

	Forward	Reverse
PCR		
S μ	GCACAGGCTCTAAATTCTGGTC	CAGGCTGGCTTCATCTTTGTCT
B2M	CGGCTCTGCTTCCCTAGAC	CGAACCGCTTGTATCACA
Mutation		
S μ	GACATGGTAAGAGACAGGCAGCCG	GGATGGAGTTGTCAATGCCAGAAA
BL2 V region	ATCTCATGTCAAGAAAATGAA	AGTCCCACCACGCAATCAT
MYC	CCCTCAACGTTAGCTCACCAACA	CGCTCAGATCCTGCAGGTACAA
SNHG3	GCCCAGGAGTGACCTATACTCAA	GGTATCCACGTTGAATGCTCA
MALAT1	GGCAGAAGGCTTTGGAAGA	CAACATATTGCCGACCTCACGGAT
BCL7A	ATTAGCTCTGGTCCGGCGGT	GGTGCAGTCGTCAAGTTCT
CUX1 ^a	GGAGGCCAGGTTGAAGGTGA	TGCCATTGGCTGTGTTCATTA
CUX1 ^b	GCTTGATCGGAAATTGATCCTC	GTCGGCGTCACCGACACAGG
CFLAR	CAGGGAAAGTGTGTTAAGTGC	CATGTTGCTCTGAAGCCAGTGC
B2M	TCTCTTCTGGCTGGAGGCTAT	AGAGGTGCTAGGACATGCGAACTT

Table S6. Gene-specific primers LM-PCR (5' to 3')

	First round	Second round
MYC 5'	CCAAGCCGCTGGTTCACTAA	GAGATAGCAGGGACTGTCCAAA
MYC 3'	GGCCCGTTAATAAGCTGCCAA	ATCCAGCCGCCACTTTGACA
SNHG3 5'	GCCCAGGAGTGACCTATACTCAA	ATGAGGCCCTCGTTGAAAA
SNHG3 3'	ACGTTGTGAAAGGACTGTACAT	TAGTGAGGAATTGAGTAACCGACA
MALAT1 5'	GCTTGAGAAGATGAGGGTGTAA	GGCAGAAGGCTTTGGAAGA
MALAT1 3'	CAACATATTGCCGACCTCACGGATT	ACACTGGCATGCTGGTCTAGGAT
BCL7A 5'	TGAGGCCCTCAAAGTGTCTCTGT	ACCAAGGGTCATTGGCAGTA
BCL7A 3'	GGTGCAGTCGTGCAAGTTCT	GGTCTCTGACTCTCCGAGTTGA
CUX1 5'	GACTCTGCCAGGTGGATGTTG	GGAGCCAGGTTGAAGGTGA
CUX1 3'	AAATGCCATTGGCTGTGTTG	TGCCATTGGCTGTGTTCATTA

Table S7. ChIP and qPCR primers (5' to 3')

	Forward	Reverse
ChIP		
V region 1	TCACCTAGGCGCCACAGGAA	CGCCACCAGCAGGGAGAAGA
V region 2	ATCTCATGTGCAAGAAAATGAAGCACCTGT	CCCTGGGATCAGAGGCAGCCTCCA
V region 3	CTCACTGGGTTTCTGTTACA	GAGCCACAGAGACAGTGCAAGTGA
V region 4	CATCAGCAGTACTAATTACTACTTGAGTTG	CGACTCTGAGGGATGGGTTGTAGT
V region 5	GTGAAGTCTCGAGACCTT	ACATGGTACTCGACTCTCG
V region 6	AGTCACCATGTCCGTAGACATGTCC	AGTCCCCCCCCTCGAGCCACTGGT
V region 7	CTGGTTGACTCTGGGGCAGGGAA	ACACTCTGACCCGAGACCTGGCA
V region 8	TGGAGGCATTTGGAGGTAGGAAA	CCAGCGAAGGAGCCCCCAGCTGC
C μ	CTTCTTCCGACTCCATCAC	CGTTCTTCTTGTGCCGT
MALAT1 1	AGAGCAGTGTAAACACTTCTGGGTG	TGGAAAGCGAGTCAAGTGGCCT
MALAT1 2	AGGTGATCGAATTCGGTGTGCGA	CAAGTCCGCTGCCCTCAGCA
MALAT1 3	CATTACTAAACGAGACGAAAATG	TTTCTCGCCTCCCGTACTCTG
MALAT1 4	TTAGAAGGTAAAGCTGAGAAGATG	AGTCCTTTAGTAGCTTTGATGTG
MALAT1 5	TTCACTGAATCTAGGAAGACAGCAG	CCTGACTCTTCTATTCACCA
MALAT1 6	GATTCCGGGTGTGTAGTTCTC	AAACCCACAAACTTGCCATCTACTA
MALAT1 7	TGGCAATTAGTGGCAGTGGCTGT	TCCATTCTAAGACTTAAGTCTCTG
MALAT1 8	TGTCTTAGGGTGGCTTTGT	GCATCTAGGCCATCATGCCAGGC
qPCR		
S μ	GACTGCAGGGAACTGGGTATCA	GGATGGAGTTGTCATGCCAGAAA
BL2 V region	GTCAGAGTCTGGAGGCATTTGG	AATGTCAGGTGAAGCGGAGAGA
MYC	GCCGCCCTCAGACTGCAT	CGGAGAGAAGGCCCTGGAGT
SNHG3	AAGCTGCCCTAGTGAACGTAGGAAG	TAGTGAGGAATTGGAGTAACCGACA
MALAT1	AAAAGGATTCAGGAAGGAGCAGT	ACACTGGCATGCTGGTAGGAT
BCL7A	CGACGCTCTAGCTCGATTGAA	GGTCAGTCTGCAAGTTCT
CUX1	TTCTGTCCCTCGGCTTCT	GCACtgAAACTCCATACCAACAA
CFLAR	AAGGGACAGGTGAGAAAGAGTAT	CTCAACTCCAGCTGACACTGCTAA
SIPA1L3	CTTGTCCAATGGATCTGTCTG	GCCGACTCAGGAACGTGTTG
KCNC2	GGGTCAAGCAATGCAACATTC	GATGCAACAGCCACTCAGTAG
ZNF451	CCTTGTCAAGATGCTCTAGTG	GCGCAACATTCACAAGCAG
TRIO	GGAAATGAGGTCTAGGGTTAAG	TGTGGATGCTAAGGAACTGAG
C5ORF13	CTCTTGGACAGCAGTTCC	GGTTTCTCCCTGCAACATCAC
CUL9	GATCCTGAGGTTAGCATACTG	TTCTGTGATCTCAAAGCTCTTC
TM9SF4	CCAGCCATGCAAAAGATGTTCC	CCTCCAGCCTCTGTGTGTT
ANKRD11	CACCAAGATCACAGCATAAGCAC	TTTGGTTGGAGACCAGCCCTTG
MYO3B	CTTGGTCCAACCCCTGTAGTTC	GAECTTGAATGATGGGCACAG
UPF2	TTGCTCTGTCAGCAATGCTC	AGAGAAGACTGCCTGGAACAAG
MET	ATGAGGCTTGAAGAGAGAGGACAAC	CACTCTGCCCTCTTCAGTTC
AUTS2	AGCTCAAGCGATTCTCCCTC	CACTCAGCACTATACCAACCAC
RAD18	GAGCCATACCAAGCAGCTGTGC	TGCAAGGGCAGTCAGTTATTAGTG
VPS13B	GTTCCTCCCTACCCACTCTAGC	TTCCAAAGGTGTCTGGGTGTATC
CCDC41	GCAAAGACAGTCAAGAGACAG	TGTGGACCTTCAGAATCCTATC
MRPL49	AGGCATCATGGAGGTACAAAC	TGGTCTGCCCTCTCAGGATTTC
NECAB3	TCACGTACCTGCCACTCAC	TTGCTTAGTTGCTGGCCCATC
SETD8	CTGAAACAGCCACAGAGTGAC	AGCAAATGGCTTGAGAAGG
SETBP1	TCTGTACCTGTGTATCTCTG	CCCATAGGTGACAAGCACCATC
PBLD	GGCCCTGATCTTGTCCATTAAAC	GCCCCGCCAATAAGAGCTTC
ABCG2	TGCCACTTATCCAGACCTAAC	ACTTACAGTTCTCAGCAGCTCTC
FAM65B	AATTGCTGGCCCGATGTAGTG	GTTTCAGTCTTGTGCCCAGG
WBSCR17	GCACTAGGTGCTGTGCAAAAC	TGCAAGCACCAGTACTCAGC
B2M	CGGCTCTGCTTCCCTAGAC	CGAAACCGCTTGTATCACAA
MAP2K4	TCTGGACATTTGGAGGAGCTCT	AAGGAAATGGTCCCTAACAGGCT
SH3KBP1	CACGTCGAGACCTGCCATTAA	GGGACTGCATGTTAGATGAGGA
TUBA1B	TCCATAACCTAGGACTATCTGA	TTGGTGGAGTGAATGACAT
RNMT	GCTGAGTCCTGAAACTTGT	GTTTGGGATTCTACAGCAAG
EXO1	GAGGATATTGCGCTGGCCAGAA	GGTCCTCAAGGCCACAGTTTCAGA

Table S8. Summary of general features of the sequenced libraries

Library	Total reads	Total mapped reads	Percent mapped reads	Unique mapping reads	Unique reads, %	Redundancy ratio
OHT(-) rep. 1	83,122,708	51,939,756	62.49	40,459,228	77.90	1.28
OHT(+) rep. 1	84,818,977	52,209,828	61.55	41,546,705	79.58	1.26
OHT(-) rep. 2	82,502,113	53,683,520	65.07	42,994,281	80.09	1.25
OHT(+) rep. 2	83,293,348	51,190,838	61.46	41,686,202	81.43	1.23